

Influence of Laser Pulse Parameters on Dynamical Processes during Azobenzene Photoisomerization

Petra Sauer and Roland E. Allen*

Department of Physics, Texas A&M University, College Station, Texas 77843

Received: February 15, 2008; Revised Manuscript Received: August 18, 2008

When a molecule is subjected to a short intense laser pulse, the ensuing dynamical processes depend qualitatively on the pulse parameters, including duration, frequency, and fluence. Here we report studies of cis to trans photoisomerization of azobenzene following femtosecond-scale laser pulses which are relatively short (10 fs) or long (100 fs) and which have a central frequency matched to either the first excited state (S_1 , or HOMO to LUMO in a molecular orbital picture) or the second (S_2 , or HOMO-1 to LUMO). The results presented here demonstrate that photoisomerization involves a rather intricate sequence of connected steps, with the nuclear and electronic degrees of freedom inextricably coupled. One important feature is the de-excitation required for the molecule to achieve its new ground-state after isomerization. If the primary excitation is to S_1 , then we find that only a single HOMO/LUMO avoided crossing is required and that this crossing occurs halfway along a rotational pathway involving the central CNNC dihedral angle. If the primary excitation is to S_2 , then the same HOMO/LUMO avoided crossing is observed, but it must be preceded by another avoided crossing that permits transfer of holes from the HOMO-1 to the HOMO, so that the HOMO is then able to accept electrons from the LUMO. We find that this earlier crossing can occur in either of two geometries, one near the cis configuration and the other near the trans. The fact that S_2 ($\pi\pi^*$) isomerization requires two steps may be related to the fact that isomerization yields are smaller for this (UV) excitation than for the S_1 ($n\pi^*$, visible-light) excitation.

I. Introduction

Azobenzene, a molecule with two phenyl rings separated by a nitrogen double bond, can isomerize when subjected to ultraviolet or visible light. Since the two distinct geometries, cis and trans, have different structural and electronic properties,¹ azobenzene has been successfully used as the parent molecule in a variety of physical, chemical, and biological molecular switching applications.^{2–9} The present work is motivated by both these potential applications and the need for a fundamental understanding of the dynamical processes responsible for isomerization.

The absorption spectrum of each isomer shows two distinct bands: one in the visible, representing excitation to the $n\pi^*$ state, and one in the UV, resulting from a $\pi\pi^*$ excitation. In *trans*-azobenzene these transitions occur near 440 and 314 nm. The first transition is symmetry-forbidden and consequently weaker. In *cis*-azobenzene both transitions are allowed, and they occur at approximately 430 and 280 nm.¹⁰

Femtosecond time-resolved spectroscopy measurements of *trans*-azobenzene in solution, and excited to the $n\pi^*$ state, indicate two transient lifetimes with values of 0.6 and 2.5 ps.¹¹ Similar measurements of *trans*-azobenzene excited to the $\pi\pi^*$ state also indicate two lifetimes, one between 0.9 and 1.2 ps and the other between 13 and 16 ps. The longer time scale was attributed to a ground-state recovery time.¹² Femtosecond transient absorption measurements on *cis*-azobenzene, excited to the $n\pi^*$ state, have produced two transient species: a dominant one with a lifetime of 170 fs, and a weaker one with a 2 ps lifetime. The ultrashort decay time of the dominant species suggests a steep potential energy surface in the vicinity of the

Franck–Condon region.¹³ Absorption measurements for *cis*-azobenzene excited to the $\pi\pi^*$ state show behavior very similar to that of *trans*-azobenzene excited to its $\pi\pi^*$ band.¹⁴

In both cases, the experimental isomerization yields are larger for excitation to the first state as compared to the second: Quantum yields in solution for trans to cis isomerization are approximately 0.24 for visible-light excitation and 0.11 for excitation with UV. The corresponding quantum yields for the cis to trans process are approximately 0.48 and 0.42.¹⁵ This difference in quantum yields has led to the suggestion that isomerization proceeds along different pathways for visible and UV excitation. One of the first ab initio calculations of the photoisomerization process in azobenzene, for the first excited state, was performed by Monti et al.¹⁶ Their multiconfigurational calculations, using a small basis set, indicate that the isomerization process proceeds along an in-plane inversion pathway, with bending through one of the central CCN bond angles. Conclusions from a later study using complete active space self-consistent field (CASSCF) methods also supported this hypothesis.¹⁷ More recently, on the other hand, calculations employing CASSCF methods,^{18–20} density-functional theory,¹³ and a semiempirical method^{21,22} show a crossing of the ground-state and first excited-state near a central dihedral angle of 90°, and a energy barrier along the inversion pathway, indicating that rotation about the central NN bond, rather than inversion, is the preferred isomerization mechanism.

Several theoretical models have also been proposed for isomerization of *cis*-azobenzene excited to the $\pi\pi^*$ state. These models include (a) a stepwise dynamics in which the molecule is quickly converted to the first excited state,¹⁴ (b) a rotational pathway on the second excited potential energy surface,²⁴ and (c) a mechanism involving a third excited singlet state ($n^2\pi^{*2}$)

* To whom correspondence should be addressed.

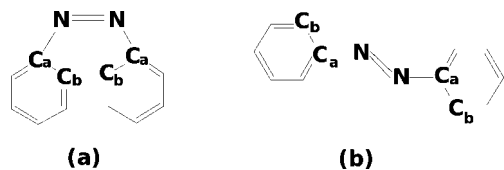


Figure 1. Equilibrated (a) cis and (b) trans conformers of azobenzene.

that has a deep minimum halfway between the cis and trans configuration along a rotational pathway.^{17,18,23}

In this paper, we present several dynamical simulations in which femtosecond-scale laser pulses with different durations, central frequencies, and fluences are applied to *cis*-azobenzene molecules that are initially in the ground state and in which isomerization is subsequently observed to occur. In these simulations, we explicitly monitor the interplay of the electronic and nuclear dynamics both during and after the excitation process, in order to clarify the influence of the laser pulse parameters and in order to reveal how the many nuclear and electronic degrees of freedom interact with one another.

II. Computational Method

In this work, we examine the dynamics of *cis*-azobenzene for several picoseconds following laser pulse excitation. These simulations require that the time-dependent Schrödinger equation be solved at each time step (typically 5 attoseconds in duration), making a fully quantum mechanical solution computationally prohibitive. (By a fully quantum solution, we mean one in which (a) all of the nuclear coordinates are treated as quantum degrees of freedom in the molecular wave function, (b) this wave function is also represented by many electronic configurations, instead of a single effective configuration, (c) the couplings between the various terms in the Born–Oppenheimer expansion below are correctly included, and (d) the molecule interacts with a radiation field which is also quantized.) As discussed below and elsewhere,^{25,26} however, a semiclassical treatment of both the nuclei and the radiation field appears to be valid in the present context. We call our approach semiclassical electron–radiation–ion dynamics (SERID) in order to emphasize its limiting approximations.²⁷ The time-dependent electronic Schrödinger equation is solved at each time step in a nonorthogonal basis set, with the Hamiltonian matrix, overlap matrix, and effective ion–ion repulsion parametrized from density functional calculations.^{28,29} As in all density-functional-based calculations, exchange and correlation effects are included only through an effective one-electron potential.

The Peierls substitution

$$H_{ab}(\mathbf{X} - \mathbf{X}') = H_{ab}^0(\mathbf{X} - \mathbf{X}') \exp\left(\frac{iq}{\hbar c} \mathbf{A}(t) \cdot (\mathbf{X} - \mathbf{X}')\right) \quad (1)$$

is used to couple the electrons to the radiation field. Here $q = -e$, \mathbf{X} is any nuclear coordinate, and $\mathbf{A}(t)$, the vector potential, is given by

$$\mathbf{A}(t) = \mathbf{A}_0 \cos\left[\frac{\pi(t - t_0/2)}{t_0}\right] \cos(\omega t) \quad (2)$$

where t_0 is the full duration of the laser pulse. With this (approximately Gaussian) form of the laser pulse, the full width at half maximum (fwhm) duration is exactly half the full duration, since the intensity is proportional to the square of the vector potential. In the discussions that follow, “duration” always

means “fwhm duration”, although the figures will display the dynamics over the full duration of the pulse, starting with $t = 0$. In the present paper, the laser pulse is always taken to have the shape defined above, but the duration, central frequency (i.e., effective photon energy), intensity (which is equivalent to fluence for a specified duration), and polarization are variable.

It should be mentioned that the present method is complementary to other methods based on different approximations. In particular, the present approach involves retaining all of the $3N_n$ nuclear degrees of freedom (where N_n is the number of atoms in the molecule), rather than discarding all but 2 or 3 which are conjectured to be most important. In addition, the present method does not assume the validity of the Born–Oppenheimer (or adiabatic) approximation, in which the various terms in the Born–Oppenheimer expansion^{30–33}

$$\Psi^{\text{tot}}(X_n, x_e, t) = \sum_i \Phi_i(X_n, t) \Psi_i(x_e, X_n) \quad (3)$$

are postulated to evolve independently of one another. In fact, the present approach includes and clearly exhibits nonadiabatic effects, which become extremely strong and of dominant importance when two or more Born–Oppenheimer terms, or “potential energy surfaces”, approach each other in energy. In the present method, this failure of the Born–Oppenheimer approximation emerges automatically during the course of a simulation, as can be seen in results like those of Figures 4, 8, and 13 in the present paper, and in many other results in our earlier papers.³⁴

These population transfers during avoided crossings, i.e., near conical intersections in the $3N_n$ dimensional space of molecular configurations,^{32,33,35} are of crucial importance in isomerization and other photochemical reactions, and the fact that they occur automatically is a major positive feature of our SERID technique. Another advantage of our method, of course, is that we include all $3N_n$ nuclear degrees of freedom. Still another is that we are able to study the effect of the properties of the laser pulse (or sequence of pulses) that is used to excite a molecule initially in its electronic ground state, whereas other widely used methods merely place the molecule in an arbitrary initial state. The effect of variations in the laser pulse parameters is, in fact, the main theme of the present paper.

III. Results and Discussion

A. Optimized Geometries. The cis and trans ground-state geometries, shown in Figure 1, were both determined in 2000 fs simulations, initiated at room temperature, in which the velocity of each atom was reduced by 0.03% at each 10 as time step. The nonplanar cis structure has C_2 symmetry and the planar trans structure C_{2h} symmetry. The relevant bond lengths, bond angles, and cohesive energies are in good agreement with both the experimental and previous ab initio results.^{13,17,18,21}

Although many molecular orbitals show some participation in the excitations described below, the HOMO-1, HOMO, and LUMO are of principal interest. Each state can be characterized by the nature of the central NN double bond when the molecule is in this state, as shown in Figure 2. The HOMO of *trans*-azobenzene is characterized by nonbonding lone pairs (represented by n), while the HOMO-1 orbital exhibits pronounced π bonding, and the LUMO π^* antibonding. Due to the nonplanarity of the ground-state of *cis*-azobenzene, the HOMO-1 and HOMO show a mix of π and n character, and the LUMO exhibits predominantly π^* antibonding character. The ground-state energies of the HOMO-1 and HOMO-2 are nearly degenerate (with a 0.11 eV energy difference in the present

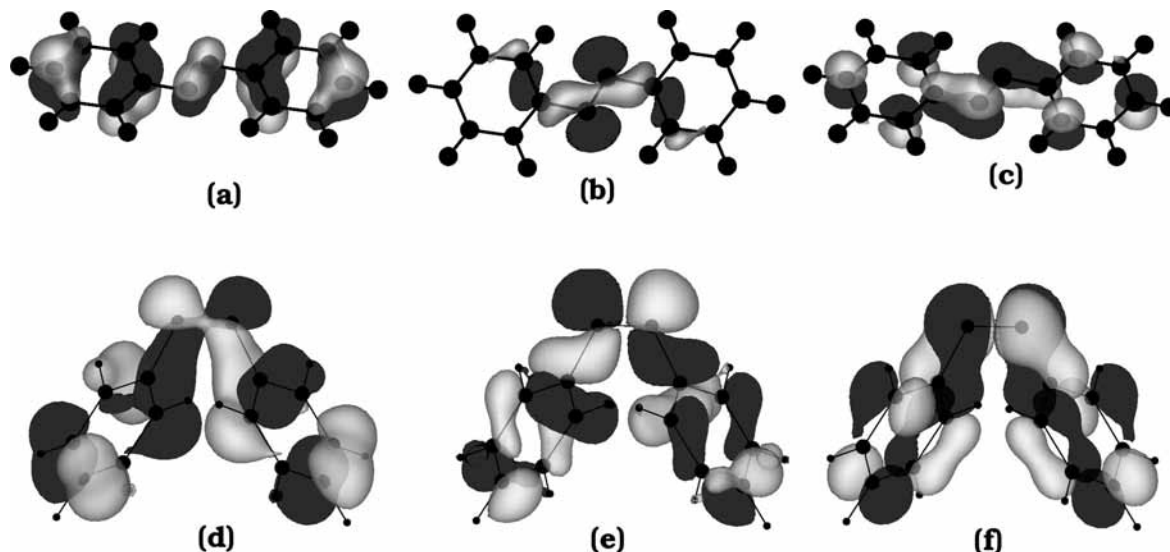


Figure 2. (a) HOMO-1, (b) HOMO, and (c) LUMO orbitals of *trans*-azobenzene. (d) HOMO-1, (e) HOMO, and (f) LUMO orbitals of *cis*-azobenzene.

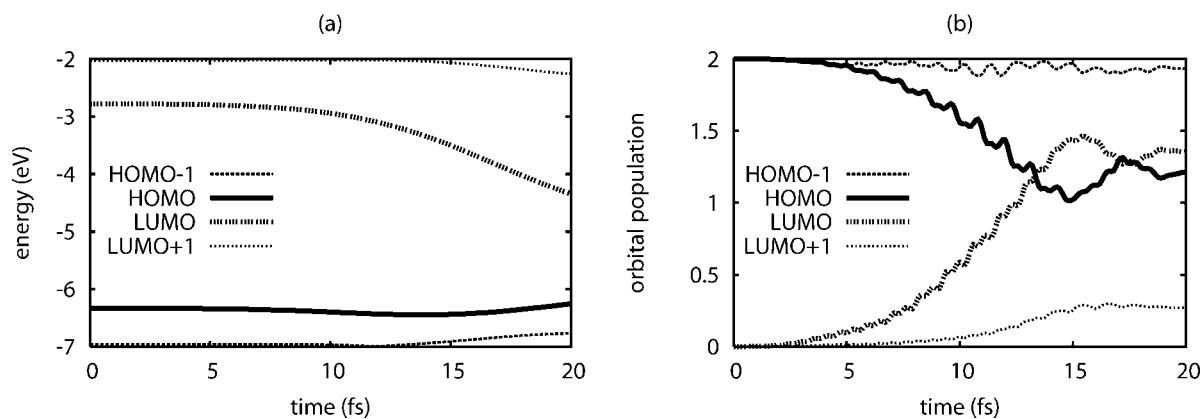


Figure 3. Changes in (a) orbital energies and (b) orbital populations of *cis*-azobenzene during excitation with a 10 fs (fwhm) laser pulse which has a fluence of 0.279 kJ/m² and an effective photon energy of 3.55 eV (matched to the ground-state HOMO–LUMO gap). The full duration of the pulse is 20 fs.

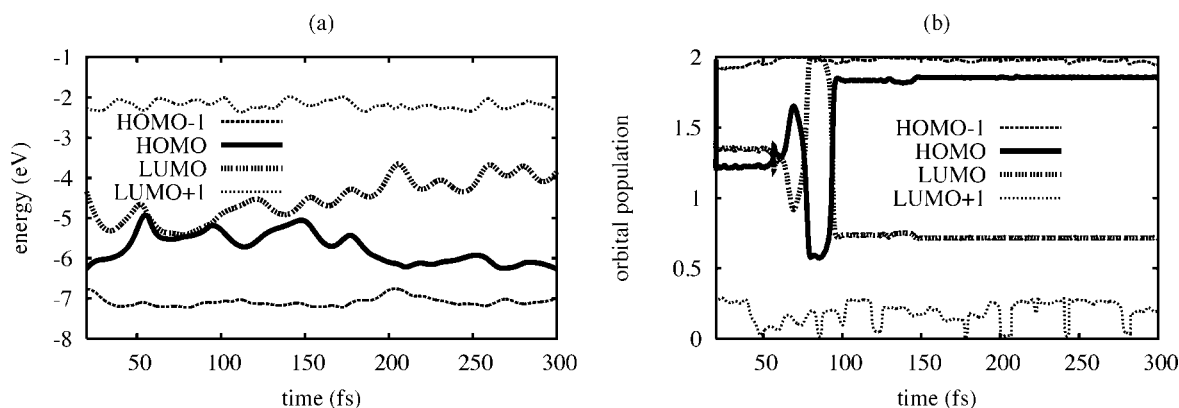


Figure 4. Changes in (a) orbital energies and (b) orbital populations for *cis*-azobenzene after excitation with a 10 fs (fwhm) laser pulse with a fluence of 0.279 kJ/m² and photon energy of 3.55 eV. The graphs begin at 20 fs, at the end of the full duration of the pulse.

density-functional-based description) and the energies of the LUMO+1 and LUMO+2 are also nearly degenerate (with only a 0.04 eV difference in energy).

B. Short Pulse Matched to HOMO–LUMO Excitation.

In order to produce an excitation that is primarily S_1 (HOMO to LUMO), a 10 fs (fwhm) pulse was applied with an effective photon energy that is matched to the equilibrated *cis*-azobenzene HOMO–LUMO gap of 3.55 eV (in the present density-

functional based model). We did not include temperature effects so that the initial state would be well-defined, and the (x,y,z) components of the vector potential were taken to be equal. Although we ran simulations for a variety of fluences, here we will show only typical results for fluences that resulted in isomerization. For the present duration and photon energy, the results shown are for a fluence of 0.279 kJ/m². With a 10 fs pulse duration, the nuclei can exhibit very little motion as the

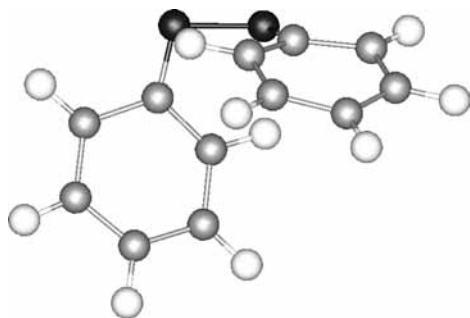


Figure 5. Geometrical structure of *cis*-azobenzene, 55 fs after irradiation with a 10 fs (fwhm) laser pulse which has a fluence of 0.279 kJ/m² and photon energy of 3.55 eV. At this time the C_aNNC_a dihedral angle has a value of 86°. With these corresponding values of the nuclear coordinates, there is an avoided crossing between the HOMO and LUMO.

electrons are initially excited, and the transitions are primarily from HOMO to LUMO, as can be seen in Figure 3. At the end of the laser pulse, the LUMO contains approximately 1.3 electrons, and the HOMO has been depleted by 0.8 electrons. This absence of an electron in an orbital that is occupied in the ground-state will be called a hole in the following discussion. There are also minor excitations out of lower-lying orbitals, and into other higher-lying orbitals, that do not play a major role in the processes described below.

The changes in electronic population induce changes in the Hellmann–Feynman forces on the nuclei and set them into motion. As the nuclei move, the bonding is modified, and the HOMO–LUMO energy gap decreases. Approximately 50–100

fs into the simulation (or 30–80 fs after the peak interaction with the radiation field), there is a series of HOMO/LUMO avoided crossings which transfer roughly 0.6 excited electrons back into the ground state, as can be seen in Figure 4. These avoided crossings occur whenever the magnitude of the central C_aNNC_a dihedral angle approaches 90°, at which point the two phenyl rings are nearly perpendicular to each other (see Figure 5). This position for the crossing is in agreement with other *ab initio* calculations, in which a conical intersection between the S₀ and S₁ states was found halfway between the *cis* and *trans* configurations along the torsional reaction coordinate^{18–22} In this simulation, there are no more avoided crossings or population transfers for the remainder of the 2000 fs simulation.

Following depopulation of the excited state, the two phenyl rings continue to rotate about the central dihedral angle, until they attain the *trans* configuration approximately 300 fs into the simulation. For the remainder of the 2000 fs simulation, the molecule exhibits small oscillations about the *trans* geometry.

For the entire duration of the simulation, both of the C_aNN bond angles oscillate between values of roughly 90° and 125°, but they never pass through a linear configuration. The nuclear dynamics, summarized in Figure 6, thus demonstrates that the isomerization mechanism is rotation rather than inversion.

C. Short Pulse Matched to HOMO-1 to LUMO Excitation. We have also simulated the response of the equilibrated *cis*-azobenzene molecule to a laser pulse which is matched to the HOMO-1 to LUMO energy difference, in order to examine the isomerization pathway for this S₂ excitation. The pulse used in the simulation discussed below has a duration of 10 fs (fwhm), a fluence of 0.148 kJ/m² and a photon energy of 4.18

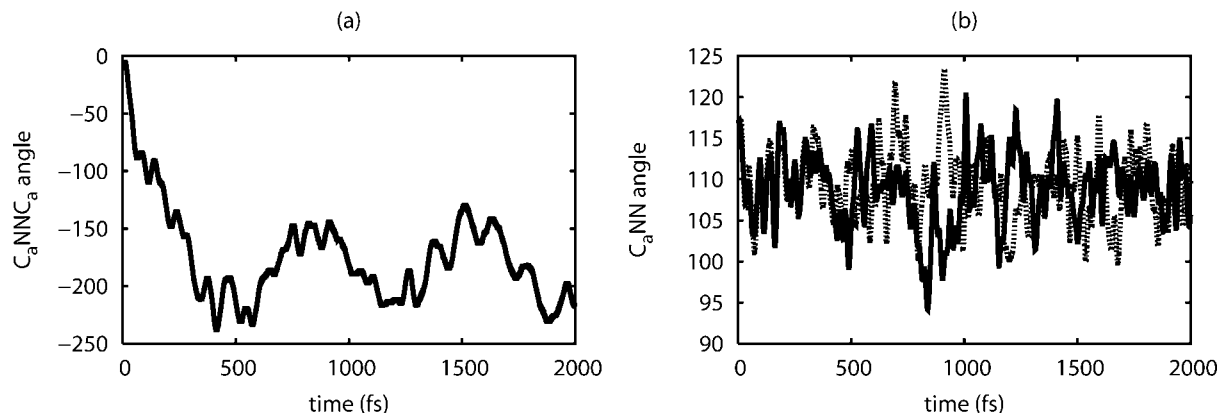


Figure 6. Dynamics of (a) the C_aNNC_a dihedral angle and (b) the two C_a NN angles of *cis*-azobenzene in response to excitation by a 10 fs (fwhm) laser pulse with a fluence of 0.279 kJ/m² and photon energy matched to the equilibrium HOMO–LUMO gap energy of 3.55 eV.

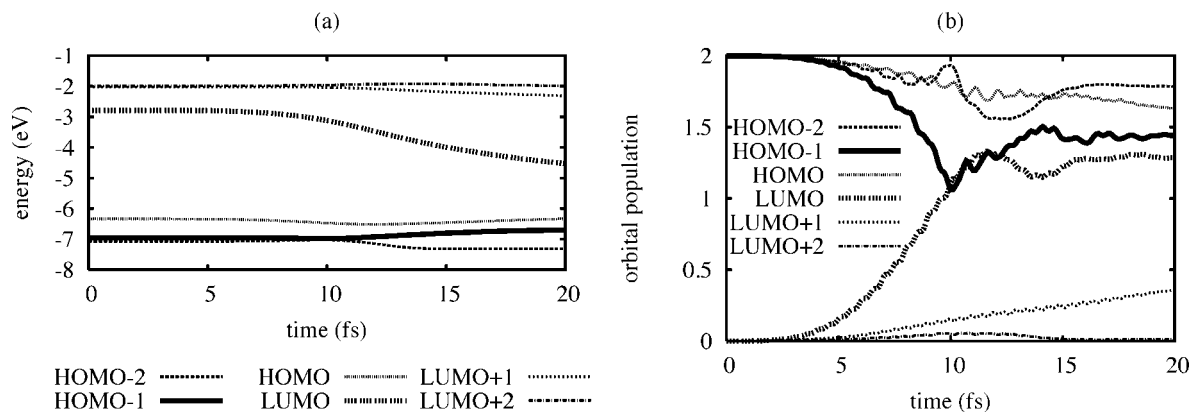


Figure 7. Changes in (a) orbital energy and (b) orbital population for *cis*-azobenzene during excitation with a 10 fs (fwhm) laser pulse with a fluence of 0.148 kJ/m² and photon energy of 4.18 eV (matched to ground-state HOMO-1 to LUMO energy difference).

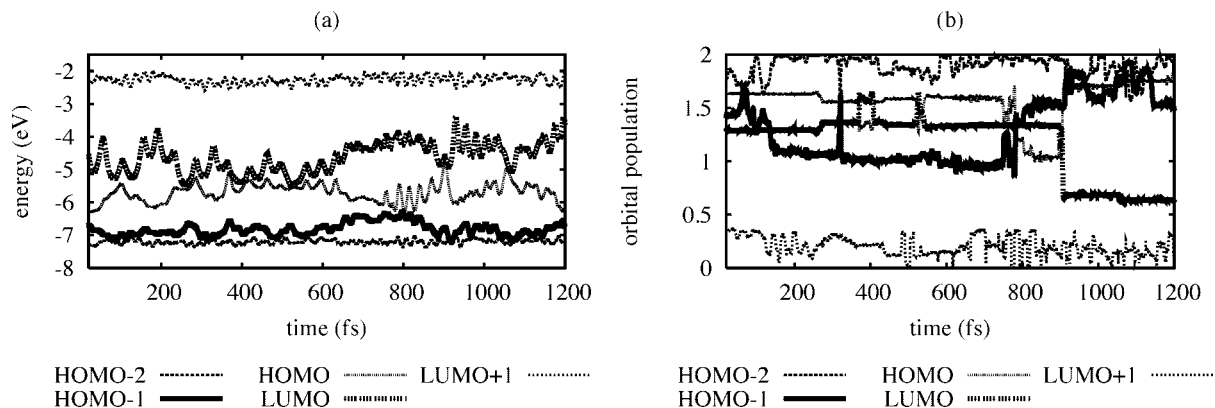


Figure 8. Changes in (a) orbital energies and (b) orbital populations of *cis*-azobenzene after excitation with a 10 fs (fwhm) laser pulse with a fluence of 0.148 kJ/m² and photon energy of 4.18 eV.

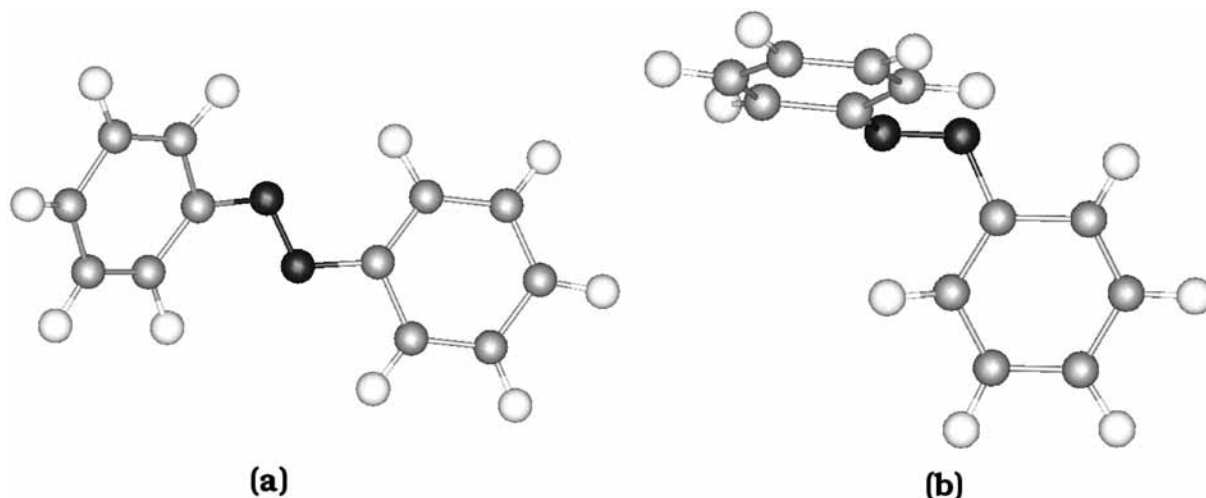


Figure 9. The structure of azobenzene (a) at 780 fs ($C_aNNC_a = 159^\circ$) and (b) 900 fs ($C_aNNC_a = 102^\circ$) in a simulation in which *cis*-azobenzene is subjected to a 10 fs (fwhm) laser pulse with a fluence of 0.148 kJ/m² and photon energy of 4.18 eV. The geometry at 780 fs occurs near a HOMO-1/HOMO avoided crossing, and the geometry at 900 fs occurs in the vicinity of a HOMO/LUMO avoided crossing.

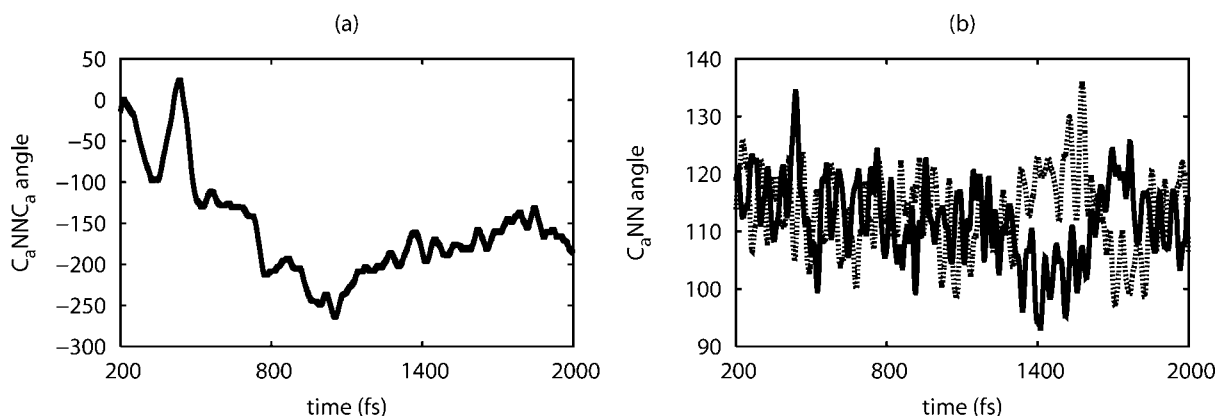


Figure 10. Variations in (a) the C_aNNC_a dihedral angle and (b) the two C_aNN angles of *cis*-azobenzene subjected to a 10 fs (fwhm) laser pulse with a fluence of 0.148 kJ/m² and photon energy matched to the HOMO-1 to LUMO energy difference of 4.18 eV.

eV. (As mentioned above, we ran several simulations for a variety of laser fluences, but here we present just one typical trajectory that resulted in isomerization.) Because of the short duration of the laser pulse, the primary excitation now is from HOMO-1 to LUMO, although there are small excitations out of the HOMO and HOMO-2 and into the LUMO+1 and LUMO+2 (see Figure 7). The near degeneracy of the higher lying unoccupied orbitals and the lower lying occupied orbitals, in conjunction with the similarity between the HOMO-1 and LUMO energy difference (4.18 eV) and the HOMO to LU-

MO+1 energy difference (4.31 eV), results in other transitions that play a negligible role in the following dynamics. At the end of the laser pulse, approximately 1.3 electrons are in the LUMO and 0.6 holes are in the HOMO-1.

The orbital energies and population for the 1.2 ps interval following excitation are shown in Figure 8. The simulation progresses without a significant electron population transfer until approximately $t = 780$ fs. At this time there is an avoided crossing between the HOMO-1 and HOMO, which transfers about 0.6 holes from the HOMO-1 into the HOMO. The

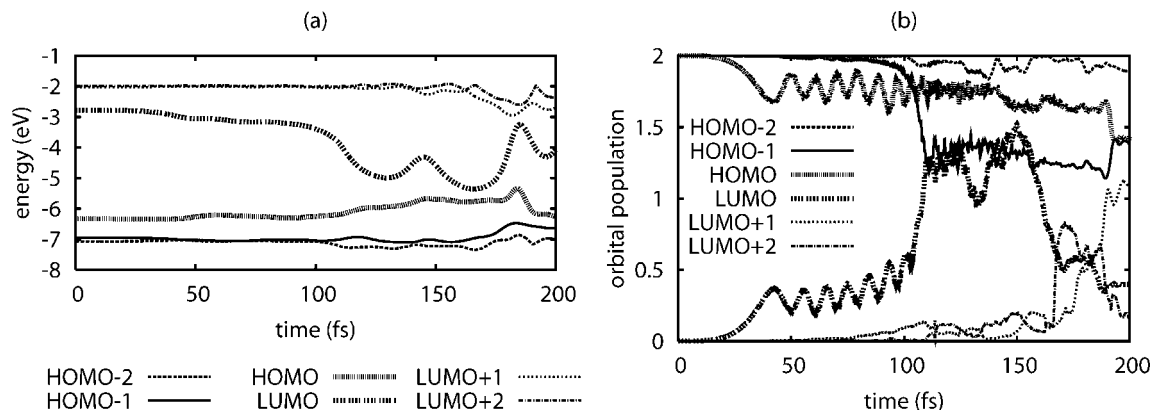


Figure 11. Changes in (a) orbital energies and (b) orbital populations of *cis*-azobenzene during excitation with a 100 fs (fwhm) laser pulse with a fluence of 0.470 kJ/m² and photon energy of 3.55 eV (matched to the ground-state HOMO–LUMO energy gap). The full duration of the pulse is 200 fs.

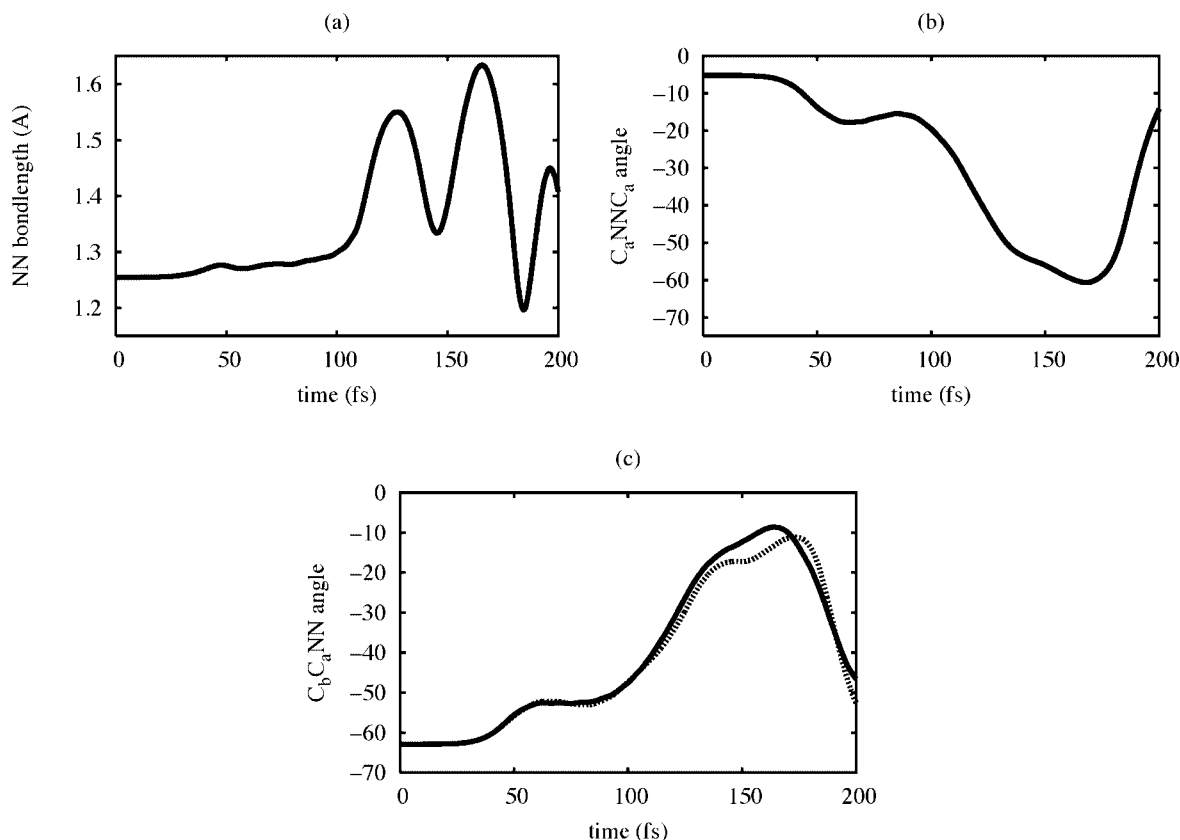


Figure 12. Variations during laser pulse excitation in (a) the NN bond length, (b) the C_aNNC_a dihedral angle, and (c) the two C_bC_aNN angles of *cis*-azobenzene, subjected to a 100 fs (fwhm) laser pulse with a fluence of 0.470 kJ/m² and photon energy matched to the HOMO–LUMO energy gap of 3.55 eV.

structure of the molecule at this time, shown in Figure 9a, indicates that the molecule is almost fully in the *trans* configuration. The geometry for this avoided crossing is similar to that of the geometry found for a *S*₂/*S*₁ conical intersection in other theoretical work.²¹

Closely following this transfer of population, at roughly 900 fs, there is an avoided crossing between HOMO and LUMO, which transfers approximately 0.7 electrons back into the ground state. This event occurs when the magnitude of the central C_aNNC_a dihedral angle approaches 90° (see Figure 9b), as in the previous case for HOMO to LUMO excitation. There are no more significant population transfers following this event.

Note that before the first major population transfer at 780 fs, there are several minor population transfers, as can be seen in

Figure 8. The first, closely following the completion of the laser pulse, is an additional transfer of holes from HOMO-2 to HOMO-1 and is due to the near degeneracy of these two orbitals. The second, a series of HOMO and LUMO avoided crossings between approximately 400 and 600 fs, does not result in a significant transfer of population back into the ground state, because the HOMO does not yet have enough holes to accommodate all of the electronic population in the LUMO. These crossings occur as the two phenyl rings are rotating through a perpendicular configuration, but do not appreciably affect the electron population dynamics.

After laser pulse excitation, the central dihedral angle of the *trans*-azobenzene tends to steadily increase in magnitude with small oscillations. As shown in Figure 10a, this dihedral angle

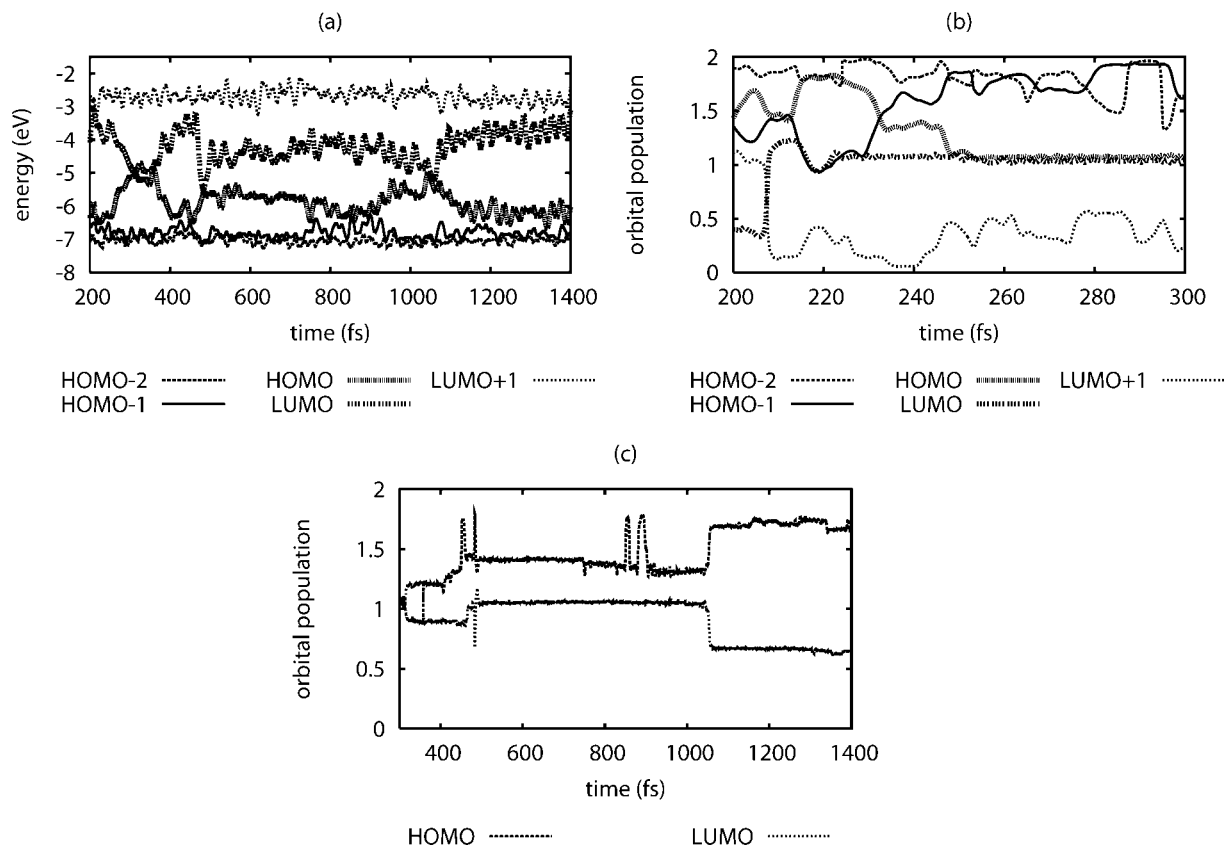


Figure 13. Changes in (a) orbital energies, (b) orbital populations between 200 and 300 fs, and (c) orbital populations between 300 and 1400 fs, following application of a 100 fs (fwhm) laser pulse with a fluence of 0.470 kJ/m² and photon energy of 3.55 eV.

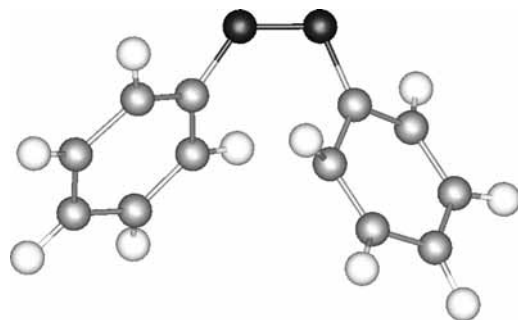


Figure 14. Structure of azobenzene molecule at 230 fs (when $C_aNNC_a = 8^\circ$) during a simulation in which *cis*-azobenzene is subjected to a 100 fs (fwhm) laser pulse with a fluence of 0.470 kJ/m² and photon energy of 3.55 eV. This geometry occurs in the vicinity of a HOMO-1/HOMO avoided crossing.

reaches the trans value at roughly 800 fs, immediately following the transfer of holes from HOMO-1 to HOMO. As in the previous case, neither of the C_aNN bond angles moves beyond 180° (Figure 10b). The isomerization mechanism for this simulation is therefore also along a rotational pathway, although it occurs entirely in an excited-state while the HOMO-1 is still significantly depopulated. Once the molecule reaches the trans configuration, the two phenyl rings continue to rotate until they reach a nearly perpendicular configuration at 900 fs (with the C_aNNC_a dihedral angle equal to approximately 270°). At this time, there is a transfer of electronic population from LUMO to HOMO, so that the molecule essentially returns to the ground state. The central dihedral angle relaxes back to the trans configuration and continues to oscillate about this position for the remainder of the 2000 fs simulation.

D. Long Pulse Matched to HOMO–LUMO Excitation.

1. Isomerization Completed in Ground State.

In order to explore the effect of nuclear motion during the laser pulse excitation, we ran simulations for a pulse with an order of magnitude longer duration, namely 100 fs (fwhm). The energy of the pulse was matched to the HOMO–LUMO gap energy of 3.55 eV, and the fluence was 0.470 kJ/m². The orbital populations and energies during application of the pulse (which has a full duration of 200 fs) are shown in Figure 11. Since the effective photon energy $\hbar\omega$ is resonant with the HOMO–LUMO transition energy (in the ground-state geometry of the molecule), electrons are initially excited out of the HOMO and into the LUMO. This change in orbital population once again induces forces on the nuclei (or ion cores), and the resulting nuclear motion again results in changes in the orbital energies, especially that of the LUMO. As the simulation progresses, the frequency of the laser pulse is no longer resonant with the HOMO to LUMO transition, and instead becomes matched to the energy difference between HOMO-1 and LUMO. The onset of a significant population transfer between HOMO-1 and LUMO begins at approximately 100 fs.

During the second half of the pulse duration, the LUMO orbital energy begins to oscillate, in response to the onset of oscillations in the central NN bondlengths (see Figure 12a). As this bond reaches maximum length, the LUMO orbital reaches minimum energy. Near the end of the laser pulse, its frequency is resonant with transitions between the LUMO and orbitals immediately above it which are closely spaced in energy. This fact, together with avoided crossings due to nuclear motion, causes a variety of population transfer processes to occur. At the end of the laser pulse, there are approximately 0.6 holes

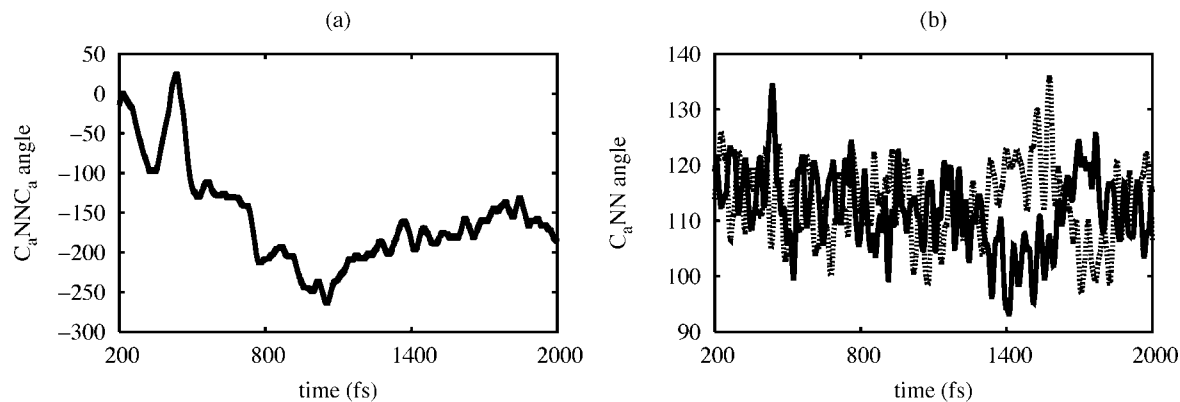


Figure 15. Variations in (a) the C_aNNC_a dihedral angle and (b) the two C_aNN bond angles of *cis*-azobenzene subjected to a 100 fs (fwhm) laser pulse with a fluence of 0.470 kJ/m^2 and photon energy matched to the HOMO to LUMO energy difference of 3.55 eV .

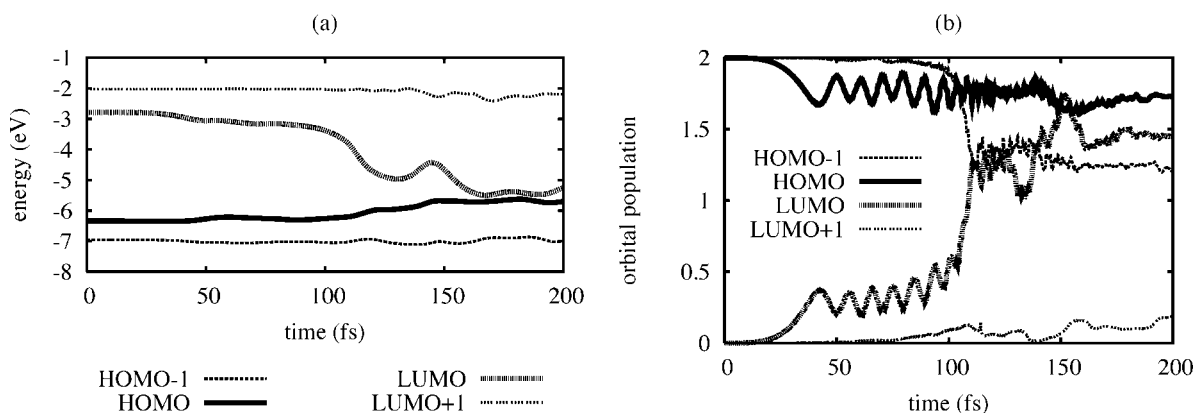


Figure 16. Changes in (a) orbital energies and (b) orbital populations of *cis*-azobenzene during excitation with a 100 fs (fwhm) laser pulse with a fluence of 0.465 kJ/m^2 and photon energy of 3.55 eV (matched to ground-state HOMO–LUMO energy gap).

in the HOMO-1, another 0.6 holes in the HOMO, 0.4 electrons in the LUMO, and 1.1 electrons in the LUMO+1.

The initial motion of the nuclei causes the two phenyl rings to rotate around the central NN bond. Their motion is such that it (i) increases the magnitude of the central dihedral angle (see Figure 12b) and (ii) brings each of the two rings separately into a more planar configuration, in the sense that the ring and its adjacent CNN angle essentially lie in one plane (see Figure 12). Initially the molecule tends to a more *trans*-like geometry. However, near the end of the initial excitation phase (i.e., application of the laser pulse), the magnitude of the central C_aNNC_a angle reaches a maximum value, and then rotates in the opposite direction, toward the starting configuration. In conjunction with this, the magnitudes of the two C_bC_aNN dihedral angles once again begin to grow. At the end of the pulse, the central dihedral angle is decreasing in size, the two phenyl rings are twisting out of the plane that they form with the central NN bond, and the molecule is moving back toward a *cis*-like geometry.

Figure 13a shows the series of avoided crossings that occur following excitation by the radiation field. The first population transfer occurs almost immediately, roughly 208 fs into the simulation, and it transfers the majority of the electrons from the higher lying orbitals back into the LUMO (Figure 13b). At this point the LUMO holds approximately 1.1 electrons. The next significant population transfer, occurring at roughly 230 fs, is due to an avoided crossing between HOMO-1 and HOMO, and it transfers approximately 0.7 holes into the highest occupied orbital (Figure 13b). This crossing occurs for a molecular geometry close to that of the starting *cis* geometry (see Figure

14), in agreement with other *ab initio* calculations in which an S_2/S_1 conical intersection has been found for *cis*-like geometries.²¹

Following the initial avoided crossings, there is roughly 1 hole in the HOMO and 1 electron in the LUMO. Between approximately 310 and 1050 fs, there is then a series of HOMO–LUMO avoided crossings which transfer a net of approximately 0.7 electrons back into the ground state (Figure 13c). Each avoided crossing occurs for a central dihedral angle of about 90° . During this time, the LUMO occasionally comes into contact with the higher lying orbitals, permitting a transfer of electrons into this state. The LUMO is therefore not entirely depopulated at 1050 fs. Following these events there are no more significant population transfers.

As can be seen in Figure 15, the molecule isomerizes from *cis* to *trans* along a rotational rather than inversion pathway. The central C_aNNC_a dihedral angle first reaches the fully *trans* value of 180° approximately 750 fs into the simulation. It then continues to rotate past this value, until approximately 1050 fs into the simulation, at which point the two phenyl rings are nearly perpendicular to each other (C_aNNC_a angle of $\sim 270^\circ$). This coincides with the avoided crossing between HOMO and LUMO, and the consequent return of the molecule to its ground state. The C_aNNC_a angle then turns around and rotates back toward the *trans* configuration, and oscillates about this configuration for the remainder of the 2000 fs simulation. At no time during the simulation do either of the C_aNN angles pass through a linear configuration (Figure 15b), demonstrating that inversion does not occur.

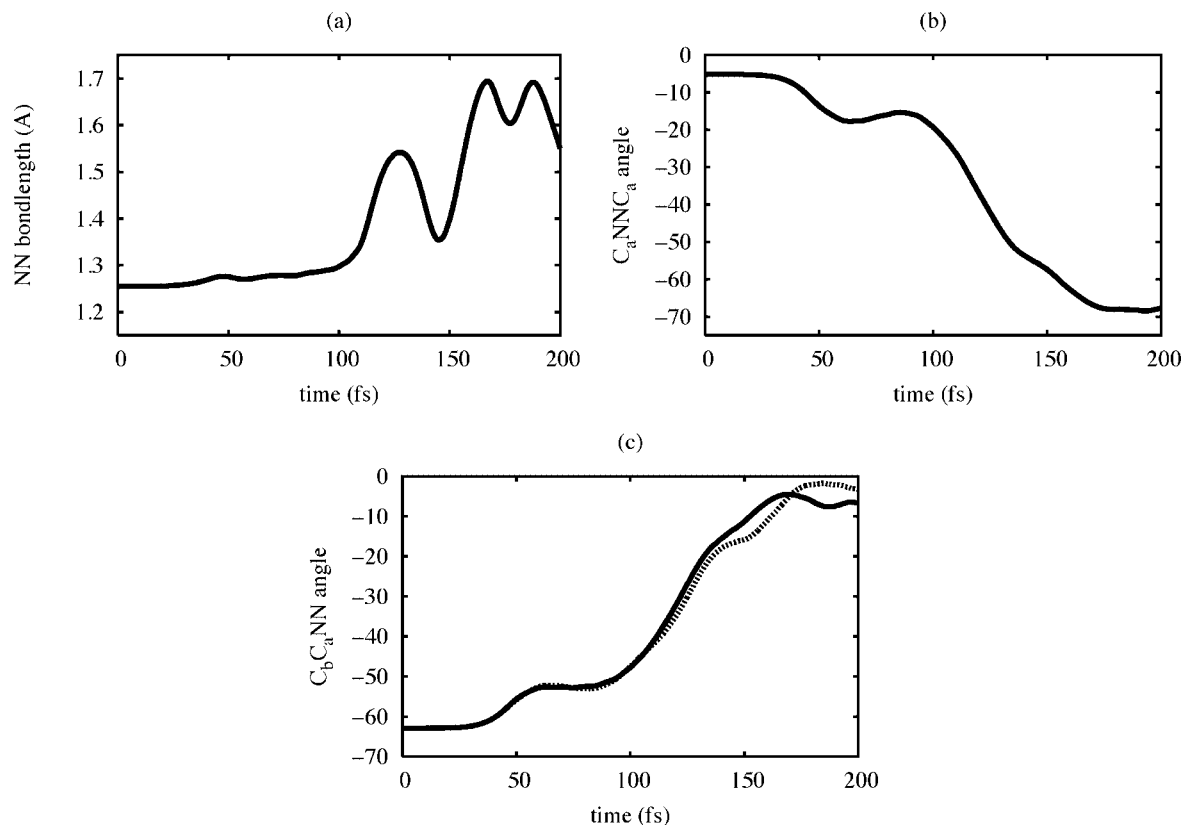


Figure 17. Variations during laser pulse excitation in (a) the NN bond length, (b) the C_aNNC_a dihedral angle, and (c) the two C_bC_aNN bond angles of *cis*-azobenzene subjected to a 100 fs (fwhm) laser pulse with a fluence of 0.465 kJ/m^2 and photon energy matched to the HOMO–LUMO gap of 3.55 eV .

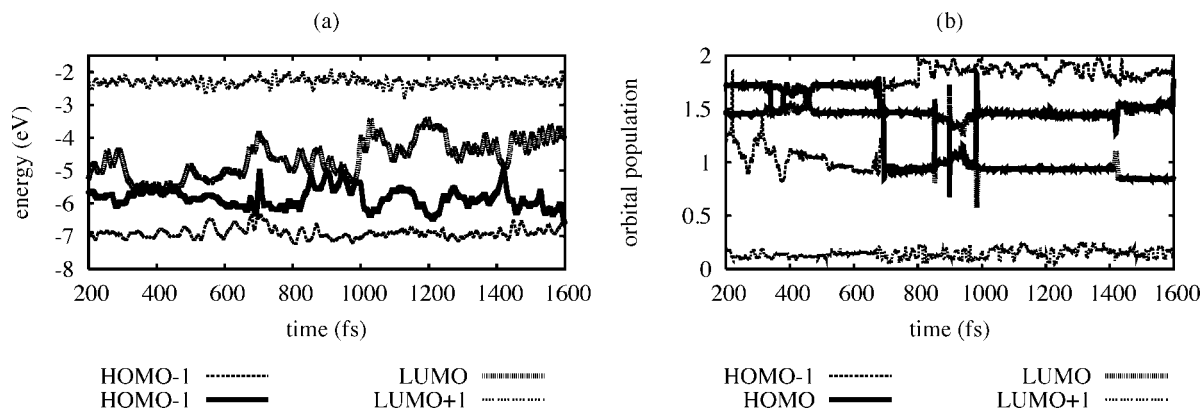


Figure 18. Changes in (a) orbital energies and (b) orbital populations after excitation with a 100 fs (fwhm) laser pulse with a fluence of 0.465 kJ/m^2 and photon energy of 3.55 eV .

In this simulation, the laser pulse excites electrons into the LUMO from both the HOMO and the HOMO-1. Almost immediately following the laser excitation, there is an avoided crossing between HOMO-1 and HOMO (while the molecule is near the *cis* configuration) that transfers the majority of the holes into the HOMO. The molecule then follows a rotational pathway toward the *trans* configuration. At a geometry halfway between the *cis* and *trans* configuration, there is an avoided crossing between HOMO and LUMO which returns the molecule to the ground state. It then continues to rotate toward the *trans* configuration in the ground state. This mechanism is similar to that described above for an ultrashort 10 fs (fwhm) pulse matched to the HOMO–LUMO gap, in that the isomerization is completed in the ground, rather than excited, state.

2. Isomerization Completed in Excited State. After the simulation discussed immediately above, we slightly decreased

the laser pulse fluence to 0.465 kJ/m^2 while keeping the other pulse parameters the same (i.e., 100 fs duration and photon energy $\hbar\omega = 3.55 \text{ eV}$). Once again, the initial excitation is out of the HOMO and into the LUMO, but nuclear motion during the remainder of the full pulse duration of 200 fs substantially modifies the orbital energies, causing sizable excitation from HOMO-1 to LUMO (Figure 16). At the end of the pulse, there are approximately 1.4 electrons in the LUMO, 0.3 holes in the HOMO, and 0.6 holes in the HOMO-1. Again, there are additionally electrons in other higher lying states, and holes in lower lying states, that do not play a major role.

A significant difference between this simulation and the previous one can be seen in the motion of the nuclei during excitation. Initially, this motion appears similar to that in the previous simulation: Oscillations are induced in the central NN bond (Figure 17a), the magnitude of the central C_aNNC_a

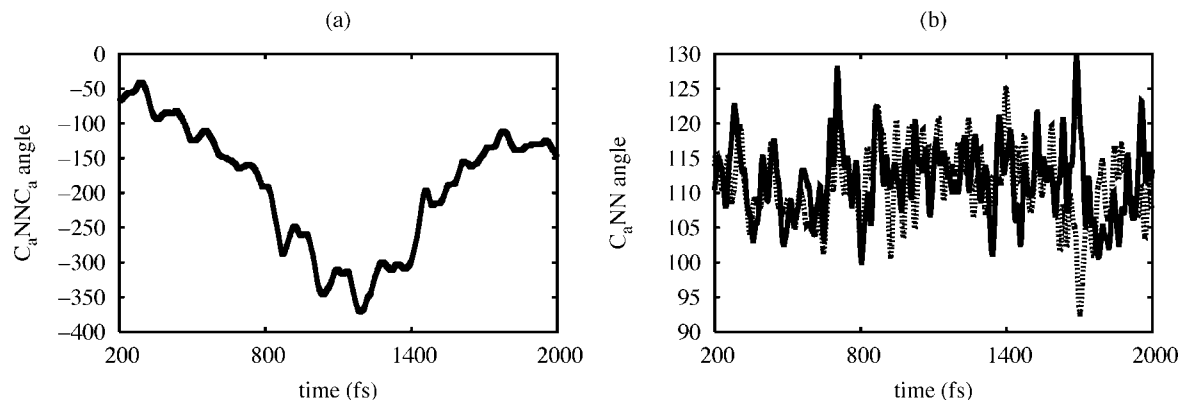


Figure 19. Variations in (a) the C_aNNC_a dihedral angle and (b) the two C_aNN bond angles of *cis*-azobenzene subjected to a 100 fs (fwhm) laser pulse with a fluence of 0.465 kJ/m^2 and photon energy matched to the HOMO–LUMO gap of 3.55 eV .

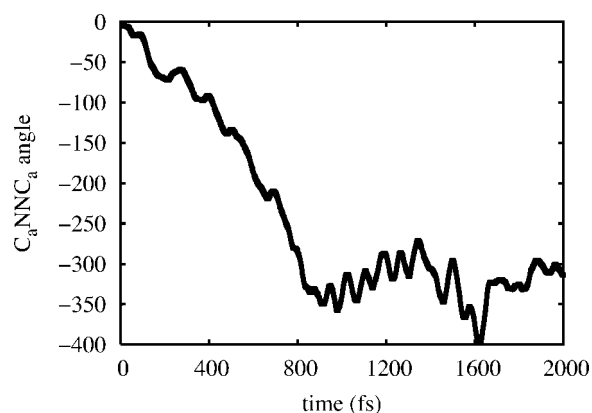


Figure 20. Variations in C_aNNC_a dihedral angle of *cis*-azobenzene subjected to a 100 fs (fwhm) laser pulse with a fluence of 0.462 kJ/m^2 and photon energy matched to the HOMO–LUMO gap of 3.55 eV .

dihedral angle grows (Figure 17b), and the magnitudes of the two C_bC_aNN angles decrease (Figure 17c). However, during the excitation, these last dihedral angles never reach the same turning point, and at the end of the laser pulse the molecule is still moving to a trans geometry.

It continues to move toward the trans geometry, with no significant population transfers until approximately 690 fs, at which time there is a HOMO-1/HOMO avoided crossing which transfers about 0.8 holes from the HOMO-1 into the HOMO (Figure 18). At this point, the geometry of the molecule is close to the trans configuration (just as for the above case of a 10 fs pulse matched to the HOMO-1 \rightarrow LUMO excitation energy). The isomerization process occurs almost entirely while the HOMO-1 contains a majority of the holes. This process is then followed by a series of HOMO/LUMO avoided crossings between about 850 and 1420 fs, which transfer approximately 0.6 electrons out of the LUMO, effectively returning the molecule to the ground state.

Each HOMO/LUMO avoided crossing occurs when the magnitude of the C_aNNC_a dihedral angle approaches 90° (Figure 19a). During the time interval between 850 and 1420 fs, the two phenyl rings rotate through this perpendicular configuration, into a *cis* configuration, back through the perpendicular configuration, and then finally into the trans configuration. As in all other simulations, the two C_aNN angles show no indication that the molecule follows an inversion pathway (Figure 19b).

As in the previous simulation for a 100 fs pulse, electrons are excited out of both HOMO-1 and HOMO, even though the pulse is initially resonant with the HOMO–LUMO gap. In this simulation, however, the molecule fully isomerizes to the trans

configuration before reaching the HOMO-1/HOMO avoided crossing that transfers the hole population from HOMO-1 to HOMO. The isomerization is completed in the excited state, rather than ground state. The electrons are then returned to the ground-state through a series of HOMO/LUMO avoided crossings. This isomerization mechanism is thus similar to that for the 10 fs pulse discussed above that was matched to the energy difference between HOMO-1 and LUMO.

Finally, we briefly discuss a typical simulation that does not result in isomerization, in which the laser fluence was slightly lower: 0.462 kJ/m^2 . In this case the electron dynamics appears similar, but the nuclear dynamics following the final HOMO/LUMO avoided crossing is different. With this fluence, the two phenyl rings of the molecule rotate from the trans geometry, through the perpendicular configuration, into the *cis* configuration and back into the perpendicular configuration, as shown in Figure 20. At this point there is a HOMO/LUMO avoided crossing that returns the molecule to the ground state. Rather than continuing on to the trans geometry, as for the pulse with a fluence of 0.465 kJ/m^2 , the molecule returns to the *cis* configuration. Following the series of HOMO/LUMO avoided crossings that return azobenzene to the ground state, there are thus two possible pathways, one leading on to the trans structure and the other back to the *cis*.

IV. Conclusions

Here we have presented detailed results for an important photochemical reaction: *cis* to trans isomerization of azobenzene, induced by laser pulses with varying duration, frequency (or effective photon energy), and fluence, in which we explicitly monitor the interaction of the nuclear motion with the electronic energies and populations. These interactions are especially important in the vicinity of three types of avoided crossings accessed by the molecule as the atoms move: a HOMO/LUMO avoided crossing that occurs approximately halfway along a rotational pathway between the *cis* and trans configurations; a HOMO-1/HOMO avoided crossing near the *cis* configuration; and another HOMO/HOMO-1 avoided crossing near the trans geometry. Different laser pulse parameters result in motion toward or away from each of these regions. Additionally, once a population transfer at an avoided crossing does occur, the molecule can follow different pathways for nuclear motion which are also controlled by the initial excitations resulting from the laser pulse.

An ultrashort 10 fs pulse excites the electronic transition too quickly for the nuclei to exhibit significant motion while the pulse is still being applied. In this case, the excitation is primarily

between two molecular orbitals whose initial energy difference is resonant with the applied laser pulse. A pulse matched to the HOMO–LUMO energy difference induces isomerization along a rotational pathway in which the molecule is returned to the ground-state through a HOMO/LUMO avoided crossing halfway between the cis and trans configurations. A laser pulse matched to the HOMO-1 to LUMO energy difference also results in isomerization along a rotational pathway. In this case however, the molecule entirely transforms to the trans state before encountering a HOMO-1/HOMO avoided crossing, followed by a series of HOMO/LUMO avoided crossings which ultimately return the molecule to the ground state.

Nuclear motion during excitation with a longer 100 fs laser pulse, matched to the HOMO–LUMO gap energy, results in a significant hole population in both the HOMO and the HOMO-1, and an electron population in the LUMO. To return to the ground state, the hole population must be transferred from the HOMO-1 to the HOMO through an avoided crossing which can occur for either a cis-like or a trans-like geometry. Both are followed by a HOMO/LUMO avoided crossing which permits a transition from the excited-state back to the ground state. The specifics of the laser pulse parameters determine which HOMO-1/HOMO avoided crossings are encountered. In the present simulations, a fluence of 0.465 kJ/m² led to an avoided crossing near the trans geometry, while a fluence of 0.470 kJ/m² resulted in an avoided crossing near the cis geometry.

Because of the complex nature of the excited-state energy surfaces of azobenzene, there are a variety of pathways that can lead to isomerization. The exact trajectory followed by the molecule is therefore controlled by the applied laser pulse parameters, and simulations like those presented here provide insight into the nontrivial nature of the dynamical processes that are being controlled.

Acknowledgment. This work was supported by the Robert A. Welch Foundation (Grant A-0929). We also thank the Texas A&M University Supercomputing Facility for the use of its parallel supercomputing resources.

References and Notes

- Zhang, C.; Du, M.-H.; Cheng, H.-P.; Zhang, X.-G.; Roitberg, A. E.; Krause, J. L. *Phys. Rev. Lett.* **2004**, *92*, 158301.
- Liu, Z. F.; Hashimoto, K.; Fujishima, A. *Nature* **1990**, *347*, 658.
- Ikeda, T.; Sasaki, T.; Ichimura, K. *Nature* **1993**, *361*, 428.
- Ikeda, T.; Tsutsumi, O. *Science* **1995**, *268*, 1873.
- Hugel, T.; Holland, N. B.; Cattani, A.; Moroder, L.; Seitz, M.; Gaub, H. E. *Science* **2002**, *296*, 1103.
- Berg, R. H.; Hvilsted, S.; Ramanujam, P. S. *Nature* **1996**, *383*, 505.
- Ichimura, K.; Oh, S.-K.; Nakagawa, M. *Science* **2000**, *288*, 1624.
- Spörlein, S.; Carstens, H.; Satzger, H.; Renner, C.; Behrendt, R.; Moroder, L.; Tavan, P.; Zinth, W.; Wachtveitl, J. *Proc. Natl. Acad. Sci. U.S.A.* **2002**, *99*, 7998.
- Volgraf, M.; Gorostiza, P.; Numano, R.; Kramer, R. H.; Isacoff, E. Y.; Trauner, D. *Nature Chem. Bio.* **2006**, *2*, 47.
- Griffiths, J. *Chem. Soc. Rev.* **1972**, *1*, 481.
- Lednev, I. K.; Ye, T.-Q.; Matousek, P.; Towrie, M.; Foggi, P.; Neuwahl, F. V. R.; Umopathy, S.; Hester, R. E.; Moore, J. N. *Chem. Phys. Lett.* **1998**, *290*, 68.
- Lednev, I. K.; Ye, T.-Q.; Hester, R. E.; Moore, J. N. *J. Phys. Chem.* **1996**, *100*, 13338.
- Tiago, M.; Ismail-Beigi, S.; Louie, S. G. *J. Chem. Phys.* **2005**, *122*, 094311.
- Satzger, H.; Root, C.; Braun, M. *J. Phys. Chem. A* **2004**, *108*, 6265.
- Zimmerman, G.; Chow, L.-Y.; Paik, U.-J. *J. Am. Chem. Soc.* **1958**, *80*, 3528.
- Monti, S.; Orlandi, G.; Palmieri, P. *Chem. Phys.* **1982**, *71*, 87.
- Cattaneo, P.; Persico, M. *Phys. Chem. Chem. Phys.* **1999**, *1*, 4739.
- Ishikawa, T.; Noro, T.; Shoda, T. *J. Chem. Phys.* **2001**, *115*, 7503.
- Cembran, A.; Bernardi, F.; Garavelli, M.; Gagliardi, L.; Orlandi, G. *J. Am. Chem. Soc.* **2004**, *126*, 3234.
- Diau, E. *J. Phys. Chem. A* **2004**, *108*, 950.
- Ciminelli, C.; Granucci, G.; Persico, M. *Chem. Eur. J.* **2004**, *10*, 2327.
- Toniolo, A.; Ciminelli, C.; Persico, M.; Martinez, T. J. *J. Chem. Phys.* **2005**, *123*, 234308.
- Gagliardi, L.; Orlandi, G.; Bernardi, F.; Cembran, A.; Garavelli, M. *Theor. Chem. Acc.* **2004**, *111*, 363.
- Rau, H. *J. Photochem.* **1984**, *26*, 221.
- Dou, Y.; Torralva, B. R.; Allen, R. E. *J. Mod. Opt.* **2003**, *50*, 2615.
- Sauer, P.; Rostovtsev, Y.; Allen, R. E. *J. Chem. Phys.* **2007**, *126*, 024502.
- Li, X.; Tully, J. C.; Schlegel, H. B.; Frisch, M. J. *J. Chem. Phys.* **2005**, *123*, 084106.
- Porezag, D.; Frauenheim, Th.; Koehler, Th.; Seifert, G.; Kaschner, R. *Phys. Rev. B* **1995**, *51*, 12947.
- Sauer, P.; Allen, R. E. *J. Mod. Opt.* **2006**, *53*, 2619.
- Born, M.; Oppenheimer, J. R. *Ann. Phys. (Leipzig)* **1927**, *84*, 457.
- Born, M.; Huang, K. *The Dynamical Theory of Crystal Lattices*; Oxford University Press: London, 1954.
- Conical Intersections: Electronic Structure, Dynamics, and Spectroscopy*; Domcke, W., Yarkony, D. R., Köppel, H., Eds.; World Scientific: Singapore, 2004.
- Baer, M. *Beyond Born-Oppenheimer: Electronic Nonadiabatic Coupling Terms and Conical Intersections*; Wiley Interscience: Hoboken, 2006.
- Sauer, P.; Allen, R. E. *Chem. Phys. Lett.* **2008**, *450*, 192.
- Teller, E. *J. Phys. Chem.* **1937**, *41*, 109.

JP801347Z